Haptic Sensing Foot System for Humanoid Robot and Ground Recognition With One-Leg Balance

Kitti Suwanratchatamanee, *Student Member, IEEE*, Mitsuharu Matsumoto, *Member, IEEE*, and Shuji Hashimoto, *Member, IEEE*

***Abstract*—This paper presents a haptic sensing foot system for humanoid robot. The two different kinds of implementations are investigated: One is an active tactile sensing technique to recognize a contacting ground slope. The other is to balance the robot body with one leg for human–robot interaction. The proposed sensors are implemented on two robotic feet. Each sensing unit on each foot consists of three thin sheets of force sensitive resistors arranged triangularly with the peripheral circuits. The research objective is to produce an artifact which can be operated in a natural and intuitive manner by utilizing the control of a foot pose to keep the direction of the foot normal to the ground surface. Throughout these works, we aim to realize the tactile sensing foot to detect the ground slope for natural foot posture control in order to assist the biped walking robot to balance its body on various types of ground surfaces. In these applications, the information about the ground floor or orientation is not required in advance.**

***Index Terms*—Ground floor recognition, haptic sensor, robots, tactile sensor, human–robot interactions.**

I. Introduction

RECENTLY, a variety of reports on human–robot interaction have been published. Although most robots have vision and auditory sensors [1], haptic sensor is another important equipment to interact with human and environment [2], [3]. This paper proposes a haptic sensing system implemented on the humanoid robots' feet. Humanoid robot is a bipedal architecture mechanism which is one of the most versatile setups for walking robot. This type of robot is highly suitable for working in human environments. It should be able to operate in various environments. For instance, a humanoid robot should be able to walk on the slopes, stairs [4], and obstacles [5] to work as human substitutes or to work together with humans. However, the complex dynamics involved in the walking mechanism make this type of robot control a challenging task. To complete this task, the robot requires the sensors and the control concept of a biped robot to realize the interaction between the robot and environment [6]. Some researchers use accelerometers as a sensor for biped walking system [7]. Some researchers propose a flexible shoe system for biped robots to optimize energy consumption of the lateral plane motion [8].

Recently, there is an increasing demand on various types of sensing devices for robots to obtain the detailed object information. Although computer vision is often employed to recognize the object shape with the position and orientation, tactile sensing is an essential ability for a robot to handle an object [9]–[15]. The tactile sensor attached on the robot can sense the object surface while the robot vision cannot get the occluded surface image such as robot skin [16]. A variety of tactile sensing systems have been proposed not only for robots, but also for human–machine interfaces, force feedback, pattern recognition, and invasive surgery. For tactile or force sensing, there are a variety of techniques and sensing devices. Previous works have used strain gauges [17], electromagnetic device sensors [18], force sensitive resistors [19], capacitive tactile array [20], optical device [21], piezoelectric resonance [22], and shape memory alloy [23]. The use of 6D force sensing module located within the robot body can perform the intrinsic contact sensing task [24] and widely used in robotic. However, it is expensive and many sensing elements are necessary inside the module. These sensors are applied to the different systems.

Our idea is to use such devices with a layout specialized for object surface sensing. We have developed tactile sensor units with force sensitive resistors and applied for the active measurement of the object shape, 3-D object edge tracing a hand poses control, human–robot cooperative work, and tactile sensing of humanoid robot [25]–[32].

This paper presents a haptic foot system for humanoid robot. Two different implementations are investigated: One is an active tactile sensing technique to recognize a contacted ground slope. The proposed sensors are implemented on two robotic feet. Each foot consists of three thin sheets of force sensitive resistors arranged triangularly with the peripheral circuits. The robot sensing foot acquires the distribution of planar ground surface by arranging three force sensitive resistors triangularly. The obtained force data are used to estimate the ground slope orientation at the specific contact point and to move the robot

Manuscript received December 31, 2008; revised April 21, 2009; accepted July 2, 2009. Date of publication September 1, 2009; date of current version July 13, 2011. This work was supported in part by "Global Robot Academia" Grant-in-Aid for Global COE Program by the Ministry of Education, Culture, Sports, Science, and Technology; by "Fundamental Study for Intelligent Machine to Coexist with Nature," Research Institute for Science and Engineering, Waseda University; by CREST project "Foundation of technology supporting the creation of digital media contents" of JST; by the Grant-in-Aid for the WABOT-HOUSE Project by Gifu Prefecture; by the research Fellowships of the Japan Society for the promotion of Science for Young Scientists, DC2: 20-56621; by the research grant of Support Center for Advanced Telecommunications Technology Research; by the research grant of Foundation for the Fusion of Science and Technology; and by the Ministry of Education, Science, Sports, and Culture, Grant-in-Aid for Young Scientists (B), 20700168, 2008. The research for this paper was conducted as part of the humanoid project at the Humanoid Robotics Institute, Waseda University.

K. Suwanratchatamanee and S. Hashimoto are with the Graduate School of Advanced Science and Engineering, Waseda University, Shinjuku, Tokyo 169-8555, Japan (e-mail: kittiene@shalab.phys.waseda.ac.jp; shuji@waseda.jp).

M. Matsumoto is with the Education and Research Center for Frontier Science, The University of Electro-Communications, Chofu, Tokyo 182-8585, Japan (e-mail: mitsuharu.matsumoto@ieee.org).

Color versions of one or more of the figures in this paper are available online at http://ieeexplore.ieee.org.

Digital Object Identifier 10.1109/TIE.2009.2030217

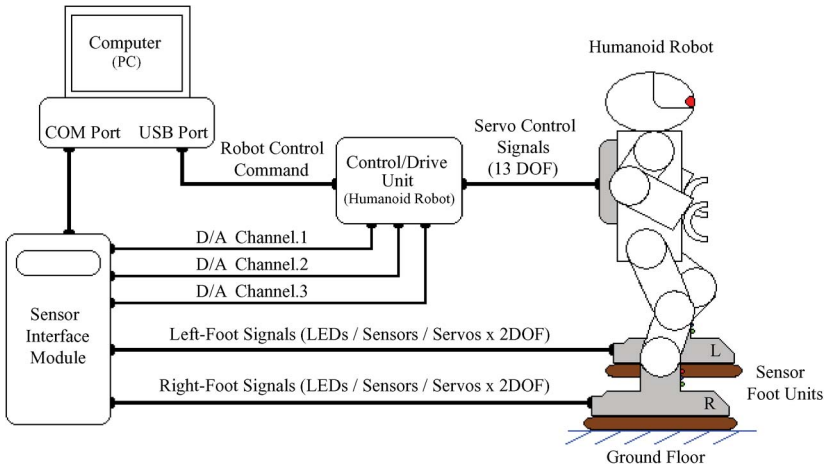

Fig. 1. Diagram of robotic tactile sensing foot system for humanoid robot.

foot normal to the ground surface for active ground slope recognition. The other is an active tactile sensing technique to recognize the strongest force position under the foot for balancing its body with one leg for human–robot interaction.

The research objective is to produce a new generation robot, which can be operated in a natural and intuitive manner instead of utilizing the complicated system. Throughout these works, we aim to realize a robotic foot with tactile sensors to detect the ground slope for natural foot posture control in order to assist the biped walking robot to balance its body on various types of ground slope such as flat level surface, up, down, left, and right slopes. In these applications, the information about the contacted ground floor or orientation is not required in advance. Important point of the proposed system is that the sensor feedback is managed locally at each foot to make the robot control distributed.

II. Tactile Sensing Foot System

The diagram of the tactile sensing foot system for humanoid robot is shown in Fig. 1. The humanoid robot can interact with the environment such as human and the ground floor. The tactile sensor units are equipped at the end of its feet. The robot is specially improved for this research based on 17-DOF humanoid robot from Kondo Kagaku Company, Ltd., "KHR-2HV."

The robot control system is separated into three parts. The main body has 13 DOF and is controlled by a personal computer (PC) through the control and the drive unit for servomotors. Another is to control two haptic sensing feet which have 2 DOF on each foot. Each robotic foot is controlled by the individual microcontroller through the sensor interface module. As our tactile sensor unit works together with the robot system, it can scan the environment space; the sensor foot unit does not require many sensing elements. The minimum number of the sensing point required for detecting the ground slope and orientation is three. The global shape measurement can be done by moving the foot along the surface of the ground.

The prepared devices are "*Flexi Force*" which is a sort of the force sensitive resistor produced by Tekscan, Inc. [33]. The diameter of the device is 9.53 mm. The device is capable of sensing forces between 0 and 4.4 N. To perform the real-time sensing process for controlling the humanoid robot, we have developed a suitable interface system. The sensor resistance decreases when the force is applied to the sensing element sheet. The resistances of three pieces of the force sensitive resistors have similar values when the force is applied to the center of all the sensing elements. Hence, by utilizing the differences between three force sensitive resistors, we can detect the gradient of the ground surface.

Fig. 2 shows the design concept and structure details of the prototype of robotic tactile sensing feet modules. Fig. 3 shows the prototype of tactile sensor feet for humanoid robot. Each foot has driver unit plugged in between microcontroller and two servomotors to give pulse signal to the 2-DOF servomotors. In addition, it provides an "alarm clock" function to synchronize the system while the microcontroller is busy with other sensing and display tasks. Interface to the driver is realized through its control and alarm signal, as shown in Fig. 4.

The three sensing devices are fixed to make triangular position. They are covered with a sponge rubber plate (soft material). We employed a sponge whose thickness is 5 mm (Young's modulus: 32.7 kPa) for the following experiments. The other side of the device is covered with a hard plate and fixed on the end effectors of each robot foot.

To simplify the functional check, the sensing devices circuit has LED indicators to show the sensing area which received the strongest force. The colors of LEDs are different to inform users the point where the force is the strongest, i.e., on the right-leg, the red color represents back touch, the green color represents front touch, the red and green colors represent the right touch, and the blue color represents left touch. It also has a liquid crystal display as well as a communication channel to send out the data to PC. The sensor signals are digitized by a resistance measuring method RC time-constant technique. Measurements are carried out in real time with developed program installed on a microcontroller and a PC.

The resistance is measured by using the charge and discharge of RC circuit, as shown in Fig. 4. After charging the capacitor, the discharge will start through the force sensitive resistor. The microprocessor measures the discharge time using the software

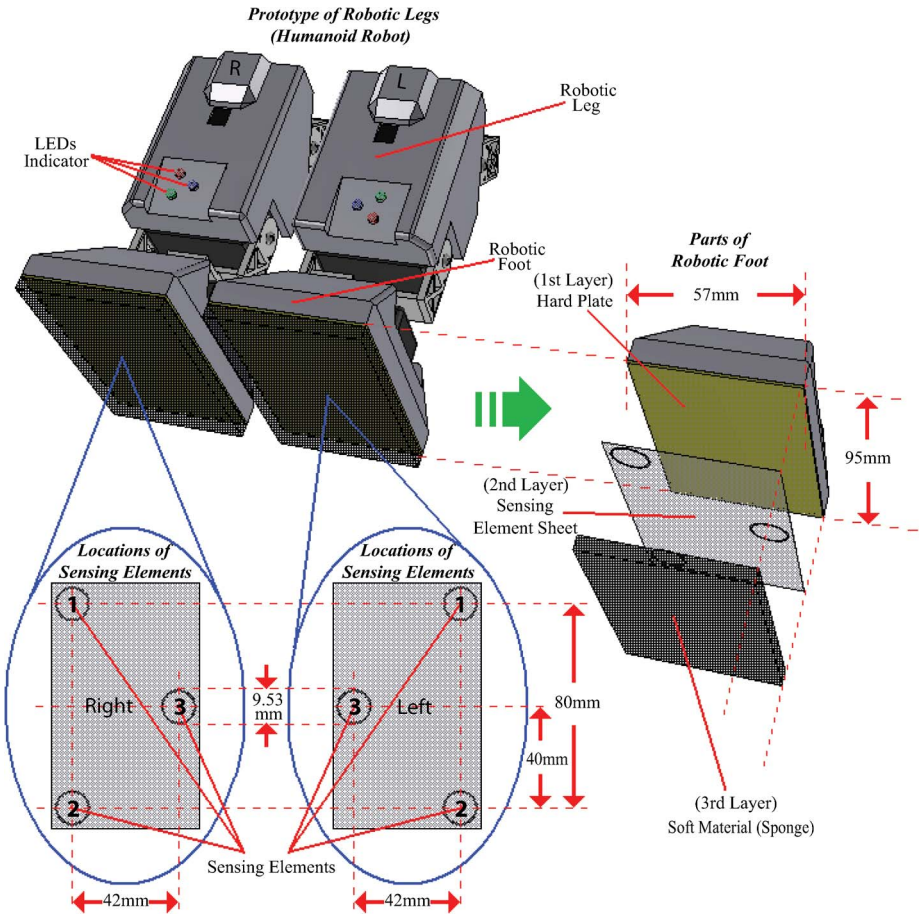

Fig. 2. Detailed structure of a prototype of tactile sensor foot for humanoid robot utilizing three element sheets.

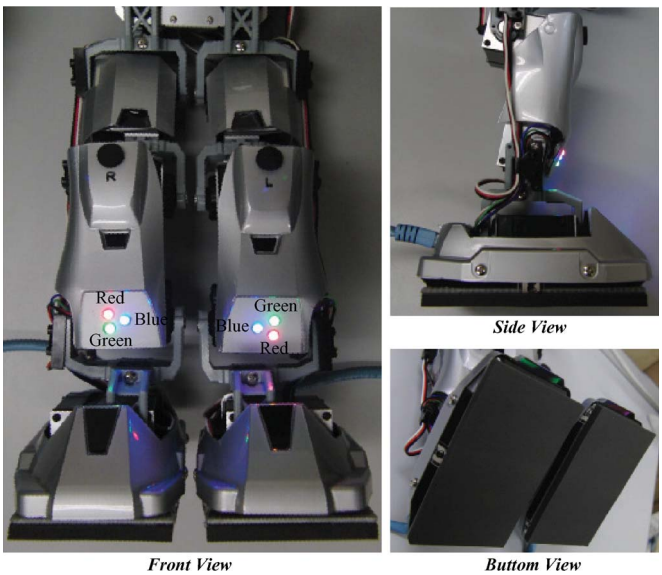

Fig. 3. Prototype of tactile sensor feet for humanoid robot.

clock counter. To measure the variable resistance of the sensing element, we utilize the RC time-constant method. The step input is applied to the circuit and the discharge time is measured. The microcontroller checks the voltage of the capacitor with 2-mS interval. To measure the discharge time of the capacitor, we estimate the time when the voltage of capacitor is less than the logic threshold voltage. The variable resistance of sensing element R can be obtained as follows:

$$R = \frac{t}{C \times \ln\left(\frac{V_{\text{Supply}}}{V_{I/O}}\right)} \tag{1}$$

where V_{Supply} and $V_{I/O}$ represent the supply voltage and the logic threshold voltage, respectively. C represents the capacitance of capacitor. t represents the discharge time. We set V_{Supply}, $V_{I/O}$, and C to 5 V, 1.4 V, and 0.01 μF, respectively.

As the maximum discharge time for each sensing element is less than 5 ms, the cycle time of the RC time measurement is short enough for the real-time control of the robot concerning each moving step. If we employ the faster robot, the more sophisticated and faster sensing method will be needed. In order to measure the variable resistance of the sensing element faster, we can also use the method by an A/D converter instead of the current method.

III. Ground Slope Sensing Method

To perform real-time sensing control for robot to adjust its foot normal to the ground surface, the control criterion is to make the receiving forces from three sensing elements equal. Note that the robot leg position is fixed. Only foot position moves followed by the received sensing information.

Fig. 5 shows a flowchart of sensing data analysis to define a contacting slope condition for robot movement control. This

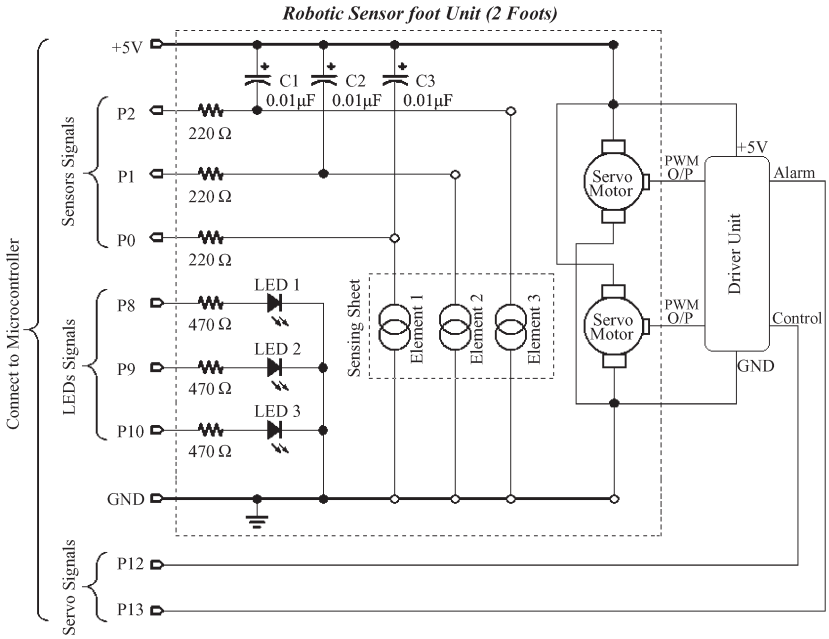

Fig. 4. Electronic circuit diagram of robotic sensor foot unit.

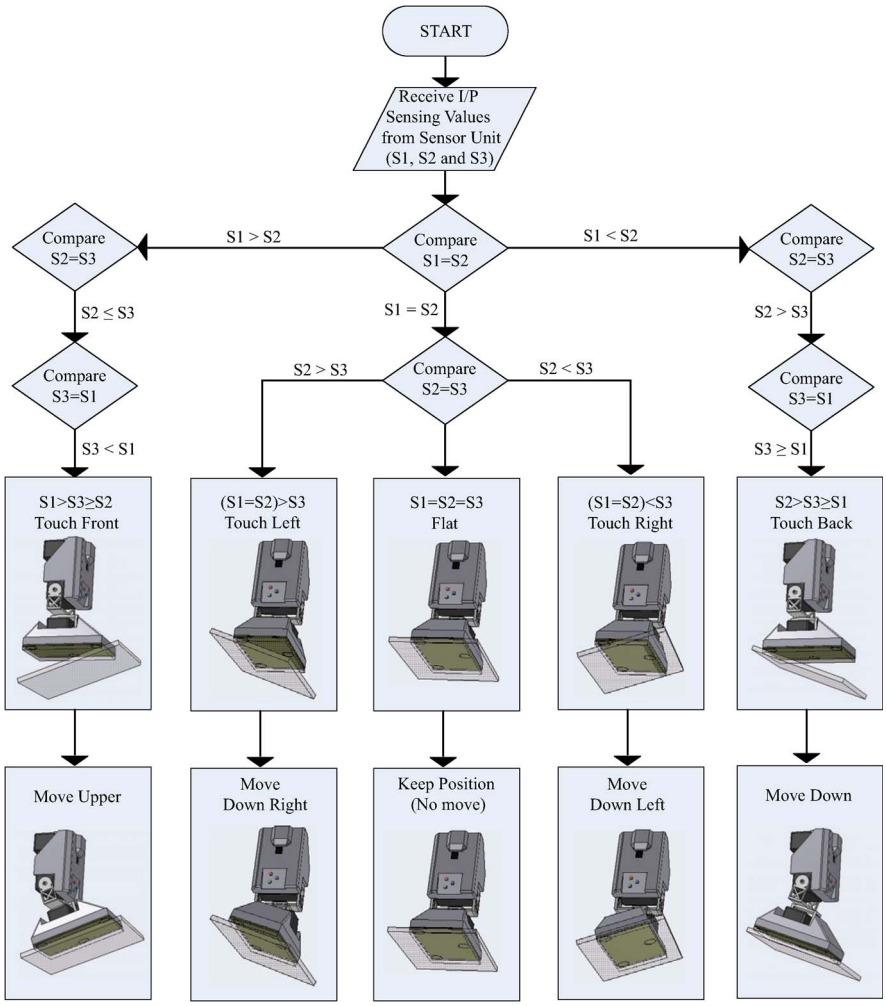

Fig. 5. Flowchart of sensing data analysis to define a contacted ground slope condition for robot movement control. (Right foot case.)

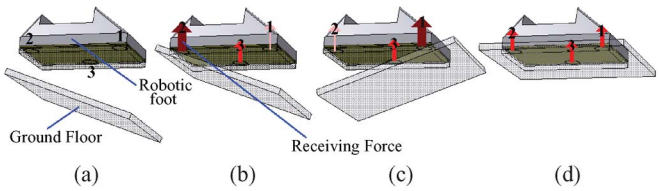

Fig. 6. Methodology of recognizing the ground floor slope. (Slope up and down.)

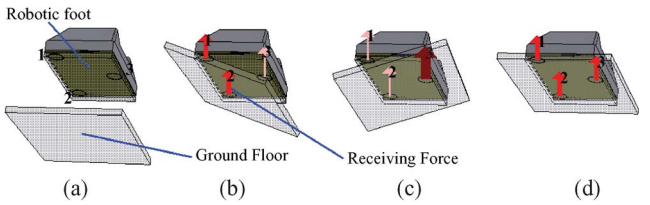

Fig. 7. Methodology of recognizing the ground floor slope. (Slope on left and right sides.)

flowchart gives an analysis example on the right foot of robot. On the left foot, the same method can also be used. However, the flowchart becomes symmetric about the right foot analysis. In Fig. 5, S_i represents the output of sensing element i ($i = 1$, 2, and 3). By using these data, we can detect the gradient of the sponge surface. To keep the robot foot normal to the ground surface, the force data from three sensor devices are used to control the robot foot direction together with the current foot direction. To complete the movement in 3-D, we introduce the four directions of movements, as shown in Fig. 5.

These figures show the analysis results of tactile sensing feedbacks to determine the robot position against the ground based on the values of the sensing elements. As shown in Fig. 5, when the robot foot touched the ground floor on the right side of the sponge, a pushing force appears on the right side. Consequently, S_3 is greater than S_1 and S_2. S_1 is equal to S_2. Hence, to follow the ground surface normal, the robot foot needs to move down left until the forces on all three sensing elements are equal. In a similar fashion, when the robot foot approaches the ground from other direction, it can also be controlled to the appropriate direction based on the sensor outputs, as shown in Fig. 5.

Fig. 6 shows the methodology of recognizing the slope in cases of up and down slopes. Fig. 6(a) shows the case that the foot has not contacted the ground and therefore no forces appear for all sensors. Fig. 6(b) shows the case that the robot foot touched the ground floor on the back side of the sponge, thus the relation between the sensor outputs is as, $S_2 > S_3 \geq S_1$. Fig. 6(c) shows the case that the robot foot touched the ground floor on the front side of the sponge, thus the relation between the sensor outputs is as, $S_1 > S_3 \geq S_2$. Fig. 6(d) shows the case that the robot foot touched normal to the ground floor, thus all forces are equal.

Fig. 7 shows the methodology of recognizing the slope in cases of left and right slopes. Fig. 7(a) shows the case that the foot has not contacted the ground and therefore no forces appear for all sensors. Fig. 7(b) shows the case that the robot foot touched the ground floor on the right side of the sponge, thus the relation between the sensor outputs is as $(S_1 \approx S_2) > S_3$. Fig. 7(c) shows the case that the robot foot touched the ground floor on the left side of the sponge, thus the relation between the sensor outputs is as $(S_1 \approx S_2) < S_3$. Fig. 7(d) shows the case that the robot foot touched normal to the ground floor, thus all forces are equal. To verify the tactile information sensing performance as a tactile interface, we created the program for analyzing the distributed pressure patterns when a robot put its foot on the ground floor. The applied force will be detected by the sensor unit and can be used for deciding the robotic foot movement automatically for assisting the robot to achieve the natural foot posture motions to be balanced on the different environments.

IV. Balance Sensing Method

To perform real-time sensing control for robot to adjust its body balanced with one leg, the control criterion is to make the receiving forces from three sensing elements equal. Note that the robot foot poses must be normal to the ground surface using previous sensing method. Its foot position is then fixed and only body pose motions are controlled by the received sensing information.

Fig. 8 shows a flowchart of sensing data analysis to define the strongest force position which appeared depending on a body movement condition. This flowchart gives an analysis example concerning the left foot of robot. On the right foot, the same method can be used. However, the flowchart becomes symmetric about the right foot analysis. In Fig. 8, S_i represents the output of sensing element i ($i = 1$, 2, and 3). By using these data, we can detect the gradient of the sponge surface. To keep the robot body balance with one leg, the force data from three sensor devices are used to control the robot body direction together with the current foot direction. To complete the movement in 3-D, we introduce the four directions of movements, as shown in Fig. 8.

The figure shows the analysis results of tactile sensing feedbacks to determine the robot position against the ground based on the values of the sensing elements. As shown in Fig. 8, when the robot moves its weight into right side of the sponge, a pushing force appears on the right side. Consequently, S_3 is smaller than S_1 and S_2, while S_1 is equal to S_2. Hence, to follow the ground surface normal, the robot needs to move its weight into left side until the forces on all three sensing elements are equal. In a similar fashion, when the robot foot approaches the ground from other direction, it can also be controlled to the appropriate direction based on the sensor outputs, as shown in Fig. 8.

Fig. 9 shows the methodology of recognizing the robot weight in cases of front and back side. In Fig. 9(a), the robot moves its weight into front side, thus the relation between the sensor outputs is as, $S_1 > S_3 \geq S_2$. Fig. 9(b) shows the robot weight in the center, thus all forces are equal. In Fig. 9(c), the robot moves its weight into back side, thus the relation between the sensor outputs is as, $S_2 > S_3 \geq S_1$.

Fig. 10 shows the methodology of recognizing the robot weight in cases of left and right side. In Fig. 10(a), the robot moves its weight into right side, thus the relation between the sensor outputs is as, $(S_1 \approx S_2) < S_3$. Fig. 10(b) shows

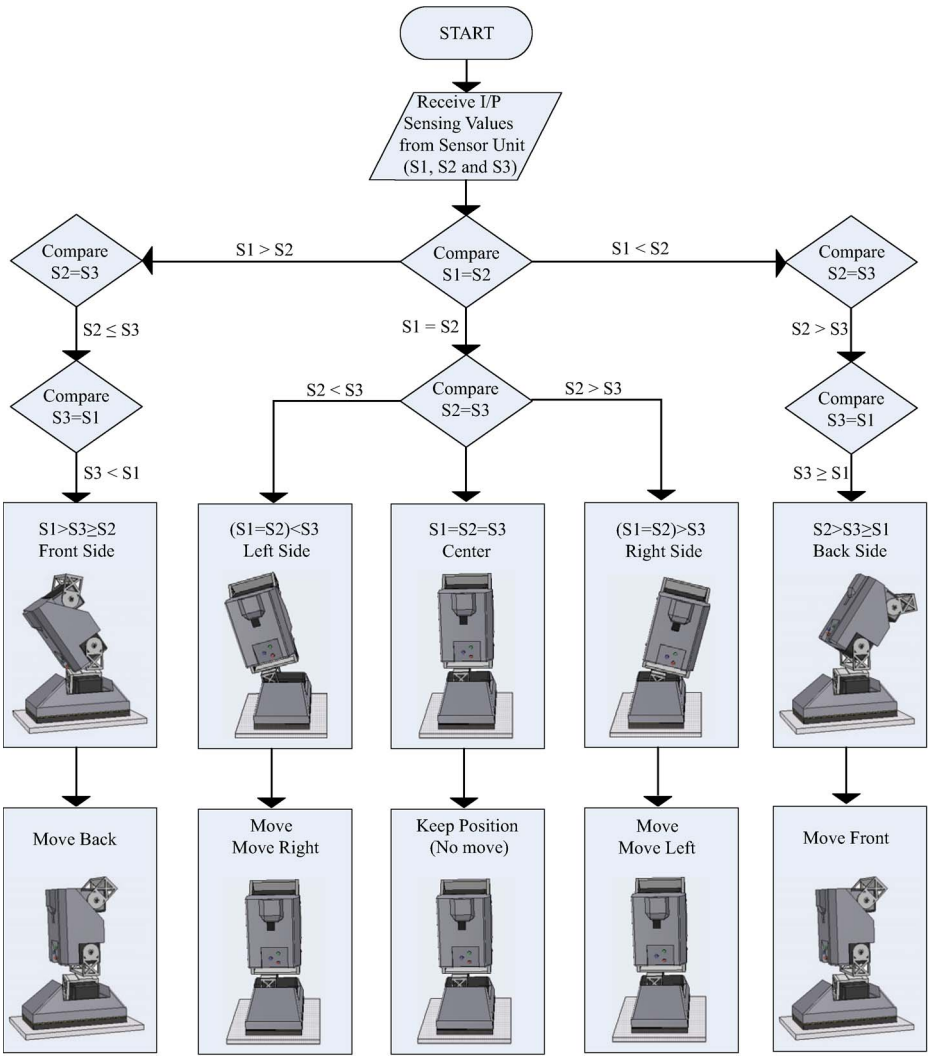

Fig. 8. Flowchart of sensing data analysis to define the strongest force position for robot balance control. (Left foot case.)

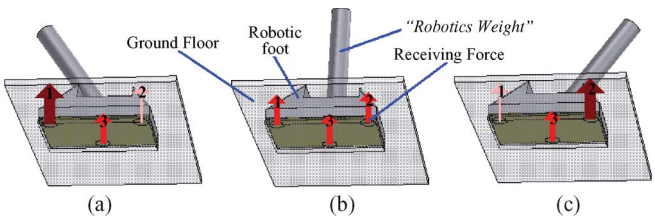

Fig. 9. Methodology of recognizing the robot weight. (Front and back.)

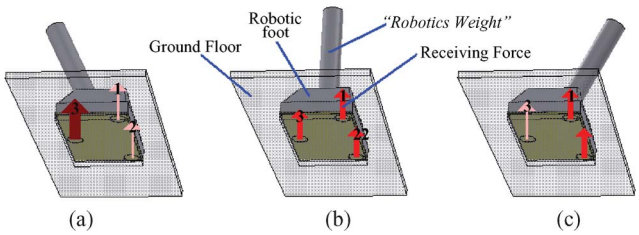

Fig. 10. Methodology of recognizing the robot weight. (Left and right.)

the robot weight in the center, thus all forces are equal. In Fig. 10(c), the robot moves its weight into left side, thus the relation between the sensor outputs is as, $(S_1 \approx S_2) > S_3$.

To verify the tactile information sensing performance as a tactile interface, we created the program for analyzing the distributed pressure patterns when a robot moves its weight along the foot. The applied force will be detected by the sensor unit and can be used for deciding the robot body movement automatically for assisting the robot to achieve the natural body poses motions to be balanced on the different ground slopes.

V. Experiment

We conducted six experiments to confirm the ability of the proposed haptic sensing foot system for controlling the motion of humanoid robot in 3-D. Two different implementations are investigated: an active tactile sensing technique to recognize a contacting ground slope by using right leg of humanoid robot is shown in the first two experiments. The one-leg balancing robot with the left leg is shown in the next four experiments. Through these experiments, we also attempted to realize effective human interaction. In particular, we apply the external force to the humanoid robot, and aim to realize the danger avoidance of humanoid robot for falling down. In these applications, we did not need any information about the contacted ground slope or orientation in advance.

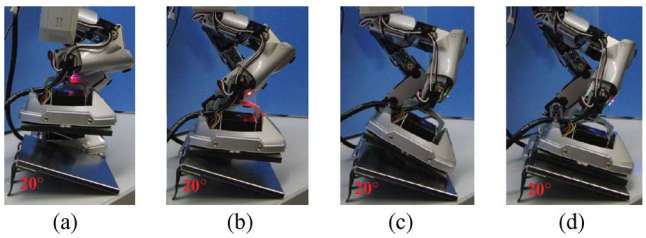

Fig. 11. Actual movement when the robot recognizes a down slope.

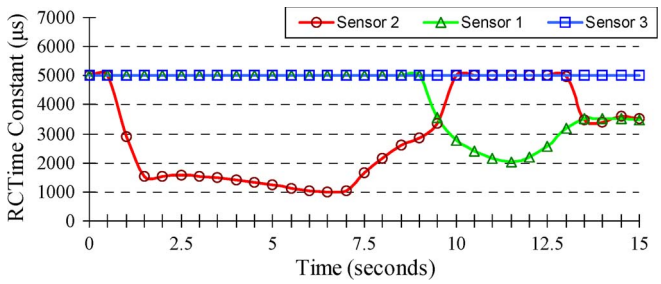

Fig. 12. Sensor data of robotic foot when the robot recognizes a down slope.

A. Experiment on Robot Foot Pose Actions (Up–Down Slope)

1) Down Slope: This experiment aims to confirm that the humanoid robot can detect down slope by using the proposed system. Fig. 11 shows the actual movement when the robot recognizes a down slope. Fig. 12 shows the sensing data of robotic foot when the robot recognizes a down slope.

The sensing data are the RC time-constant value in the RC circuit of each sensing element. When the sensor is unloaded, its value is high (unloaded case, we set maximum detecting values as 5000 μs). RC time-constant value decreases when force is applied to the sensor. In this experiment, the right foot was first set above the 20° down slope, as shown in Fig. 11(a). At this point, the sensor is unloaded, and thus all three sensing values are 5000 μs as shown at 0 s in Fig. 12. In other words, when all sensing values are maximal values, the robot foot is free from the ground. Next, the robot moved its foot down to touch the ground slope, as shown in Fig. 11(b). When the robot did this action, the sensing value on sensor 2 decreased as shown at 1.5 s in Fig. 12. After the first touch, the robot began turning its foot by utilizing the analyses of the distributed pressure patterns. In this case, the outputs of the sensor elements are constrained as follows:

$$SR_2 > SR_3 \geq SR_1 \tag{2}$$

where the SR_i represents the sensor output from the ith sensor on the right foot. To follow the ground surface normal under the aforementioned condition, the robot foot needs to turn the ankle joint forward until the forces on all three sensing elements are equal or the forces between sensor 1 and 2 are equal. These actions are shown at 9.5 s in Fig. 12. However, to confirm the correctness of the results, we temporarily controlled the robot foot to overshoot the point where the receiving forces are equal, as shown in Fig. 11(c). The graph at 10 s in Fig. 12 shows the three sensors data when the robot did the overshoot. Finally, the robot turned its foot back to the position where the receiving forces are equal, as shown in Fig. 11(d). The graph at 13.5 s in Fig. 12 shows the three sensors data when the robot did the action. Throughout this experiment, the robot can detect the ground slope and move its foot normal to the ground surface in case of following the down slope.

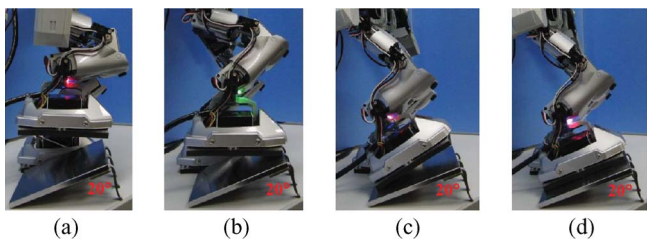

Fig. 13. Actual movement when the robot recognizes an up slope.

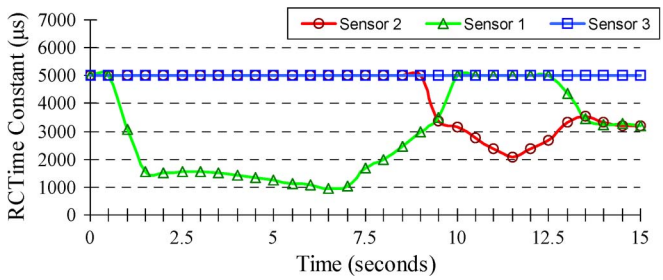

Fig. 14. Sensor data of robotic foot when the robot recognizes an up slope.

2) Up Slope: This experiment aims to confirm that the humanoid robot can detect the up slope by using the proposed system. Fig. 13 shows the actual movement when the robot recognizes an up slope. Fig. 14 shows the sensing data of robotic foot when the robot recognizes an up slope.

In this experiment, the right foot was first set above the 20° up slope, as shown in Fig. 13(a). At this point, the sensor is unloaded, thus all three sensing values are 5000 μs as shown at 0 s on Fig. 14. Next, the robot moved its foot down to touch the ground slope, as shown in Fig. 13(b). When the robot did this action, the sensing value on sensor 1 decreased as shown at 1.5 s in Fig. 14. After the first touch, the robot began turning its foot by utilizing the analyses of the distributed pressure patterns. In this case, the outputs of the sensor elements are constrained as follows:

$$SR_1 > SR_3 \geq SR_2. \tag{3}$$

Based on the sensor values, to follow the ground surface normal, the robot foot needs to turn the ankle joint backward until the forces on all three sensing elements are equal or the forces between sensor 1 and 2 are equal. These actions are shown at 9.5 s in Fig. 14. However, to confirm the correctness of the results, we temporally controlled the robot foot to overshoot the point where the receiving forces are equal, as shown in Fig. 13(c). The graph at 10 s in Fig. 14 shows the three sensors data when the robot did the overshoot. Finally, the robot turned its foot back to the position where the receiving forces are equal, as shown in Fig. 13(d). The graph at 13.5 s in Fig. 14. shows the three sensors data when the robot can detect the ground slope and move its foot normal to the ground surface in case of following the up slope.

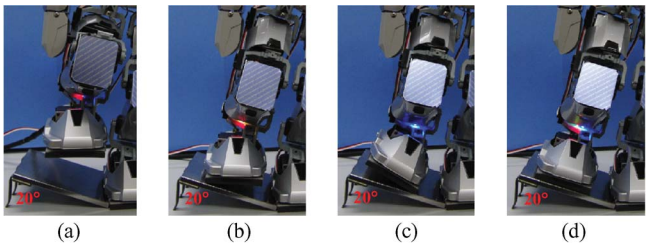

Fig. 15. Actual movement when the robot recognizes a right-side slope.

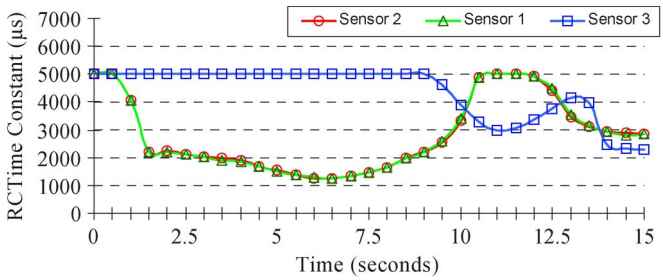

Fig. 16. Sensor data of robotic foot when the robot recognizes a right-side slope.

B. Experiment on Robot Foot Pose Actions (Left–Right Slope)

1) Right Slope: This experiment aims to confirm that the humanoid robot can detect the right slope by using the proposed system. Fig. 15 shows the actual movement when the robot recognizes a right side slope. Fig. 16 shows the sensing data of robotic foot when the robot recognizes a right-side slope. In this experiment, the right foot was first set above the 20° right-side slope, as shown in Fig. 15(a). At this point, the sensor is unloaded, and therefore all three sensing values are 5000 μs as shown at 0 s in Fig. 16. Next, the robot moved its foot down to touch the ground slope, as shown in Fig. 15(b). The graph at 1.5 s in Fig. 16 shows the three sensors data when the robot did the movement. At this point, the sensing values on sensor 1 and 2 decreased. After the first touch, the robot began turning its foot by utilizing the analyses of the distributed pressure patterns. In this case, the outputs of the sensor elements are constrained as follows:

$$(SR_1 \approx SR_2) < SR_3. \tag{4}$$

To follow the ground surface normal, the robot needs to turn the ankle joint down to the left-side until the forces on all three sensing elements are equal. The data from three sensors in the aforementioned control process are shown around 10 s in Fig. 16. However, we also temporally controlled the robot foot to overshoot the detected point, as shown in Fig. 15(c), and at 10.5 s in Fig. 16. Finally, the robot turned its foot back to the position where the receiving forces are equal, as shown in Fig. 15(d), and at 12.5 s in Fig. 16. Throughout this experiment, the robot also can detect the ground slope and move its foot normal to the ground surface in case of following the right-side slope.

2) Left Slope: This experiment aims to confirm that the humanoid robot can detect the left slope by using the proposed system. Fig. 17 shows the actual movement when the robot recognizes a left-side slope. Fig. 18 shows the sensing data

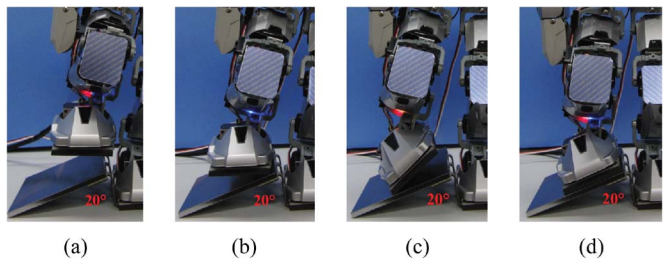

Fig. 17. Actual movement when the robot recognizes a left-side slope.

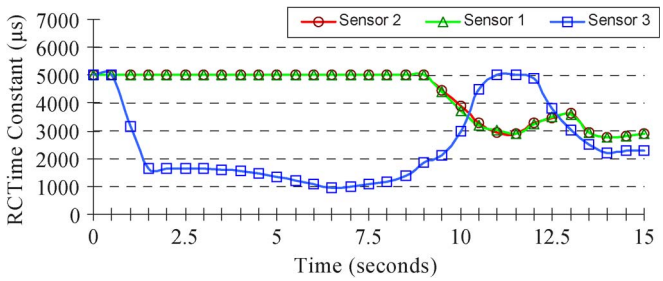

Fig. 18. Sensor data of robotic foot when the robot recognizes a left-side slope.

of robotic foot when the robot recognizes a left-side slope. In this experiment, the right foot was first set above the 20° left-side slope, as shown in Fig. 17(a). At this point, the sensor is unloaded, and therefore all three sensing values are 5000 μs as shown at 0 s on Fig. 18. Next, the robot moved its foot down to touch the ground slope, as shown in Fig. 17(b). The graph at 1.5 s in Fig. 18 shows the sensor output throughout the movement. At this point, the sensing value on sensor 3 decreased. After the first touch, the robot began turning its foot by using the analyses of the distributed pressure patterns. In this case, the outputs of the sensor elements are constrained as follows:

$$(SR_1 \approx SR_2) > SR_3. \tag{5}$$

To follow the ground surface normal, the robot foot needs to turn the ankle joint down to the right-side until the forces on all three sensing elements are equal. The sensor outputs throughout the movements are shown around 10 s in Fig. 18. However, we also temporally controlled the robot foot to overshoot the detected point, as shown in Fig. 17(c), and at 10.5 s in Fig. 18. Finally, the robot turned its foot back to the position where the receiving forces are equal, as shown in Fig. 17(d), and at 12.5 s in Fig. 18. Throughout this experiment, the robot also can detect the ground slope and move its foot normal to the ground surface in case of following the left-side slope.

C. Experiment on Robot Balance Actions (Weight on Front Side)

1) Uncontrolled Case: This experiment aims to show the failed example of the robot when the robot turn its body to the front side without the proposed method. In this procedure, first we set the robot balance with only the left leg. Then, the robot turns its body into the front side by 1° until 20° to make the robot unbalanced. As a result, after the robot turn to the front without balance control, the robot fell down to the front direction, as shown in Fig. 19(a)–(c), respectively.

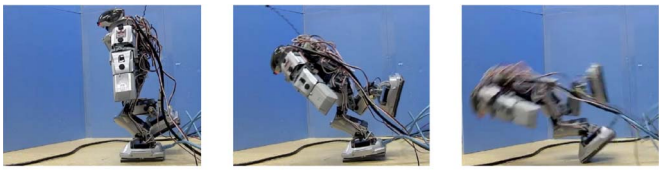

Fig. 19. Actual movement when the robot turns front. (Without balance control.)

Fig. 20. Actual movement when the robot turns front. (With balance control.)

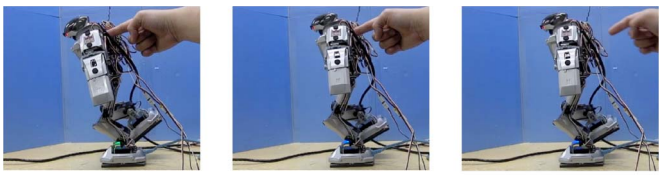

Fig. 21. Actual movement when the robot interacts with human. (Push back side.)

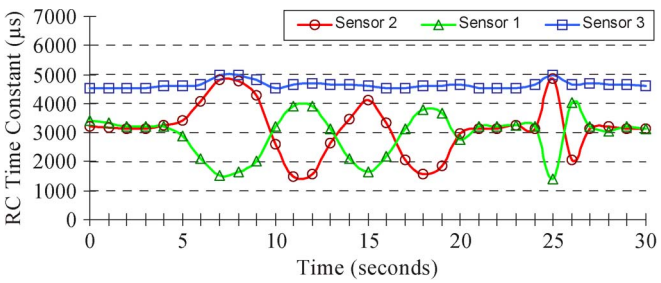

Fig. 22. Sensor data of robot foot when the robot has one-leg balance control. [Robot turns front itself (5–20 s) and human pushes back side (25 s).]

2) Controlled Case: The experiment aims to show two successful example of the balance control of the robot. One is the same unbalanced situation as the failure case. In this case, although the robot turned its body to the front side by itself the same as the previous experiment, the robot could keep its balance. The other is the unbalanced situation caused by the human.

In this experiment, human pushed the robot from the back side to realize human–machine interaction. The robot also could balance its body despite the disturbance from the human. Fig. 20 shows the actual movement of the robot when the robot turns to the front side by itself based on the sensor values. Fig. 21 shows the actual movement when the human pushes the robot from the back side. Fig. 22 shows the sensing data of this experiment. In this procedure, we first set the robot stand with only left leg in 2 s for initializing the sensing values as shown in Fig. 20(a), and between 0 and 2 s in Fig. 22. Then, the robot starts to turn its body to the front side the same as

Fig. 23. Actual movement when the robot turns back. (Without balance control.)

previous experiment to make the robot unbalanced, as shown in Fig. 20(b) and 5 s in Fig. 22. From 5 to 7 s, the robot moved to the front until it reached 3°. After that, the robot reacted to keep its balance based on the sensor values, which is different from the initial sensing values.

Hence, the minimum angle that can be detected is 3° for this balancing case. From 8 s in Fig. 22, the robot began turning its body against the internal movement by utilizing the analyses of the distributed pressure patterns. In this case, the outputs of the sensor elements are constrained as follows:

$$SL_1 > SL_3 \geq SL_2 \tag{6}$$

where the SL_i represents the sensor output from the ith sensor on the left foot. Based on the sensor values, to make its foot normal to the ground surface, the robot needs to move its body back until the robot turned to the balance position again at 10 s in Fig. 22. However, the robot is still moving to reach at 20°. Thus, the humanoid robot repeatedly turned its body to be balanced again at 13, 17, and 20 s in Fig. 22.

Finally, the robot turned to the balance position again where the receiving forces on sensor 1 and 2 are equal, as shown in Fig. 20(c). The robot keeps the balance from this point. The next experiment aims to show that the proposed system enables us to realize human–machine interaction in case that human pushes the robot from the back side. A human then applied the pushing force from the back side of robot body by using his finger, as shown in Fig. 21(a), and at 25 s in Fig. 22. The force from the human makes the robot unbalanced. At this state, the robot body began turning by utilizing the analyses of the distributed pressure patterns as described in (6). Based on the sensor values, to make the force on sensor 1 and 2 equal, the robot moves back against human, as shown in Fig. 21(b), and at 26 s in Fig. 22. Then, human leaves their finger out of the robot and the robot still maintains the balance position without falling down, as shown in Fig. 21(c), and at 27 s in Fig. 26. As shown in these figures, the robot also could keep its body based on the balance control in spite of the disturbance from the internal and external forces.

D. Experiment on Robot Balance Actions (Weight on Back Side)

1) Uncontrolled Case: This experiment aims to show the failed example of the robot when the robot turn its body to the back side without the proposed method. In this procedure, first we set the robot balance with only the left leg. Then, the robot turns its body into the back side by 1° until 20° to make the robot unbalanced. As a result, after the robot turns to the back without the balance control, the robot fell down to the back direction, as shown in Fig. 23(a)–(c), respectively.

(a) (b) (c)

Fig. 24. Actual movement when the robot turns back. (With balance control.)

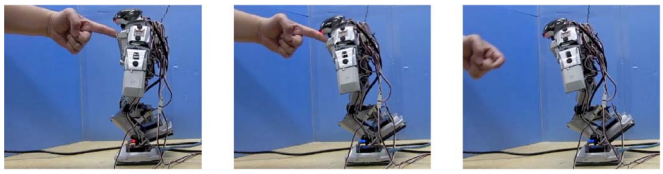

(a) (b) (c)

Fig. 25. Actual movement when the robot interacts with human. (Push front side.)

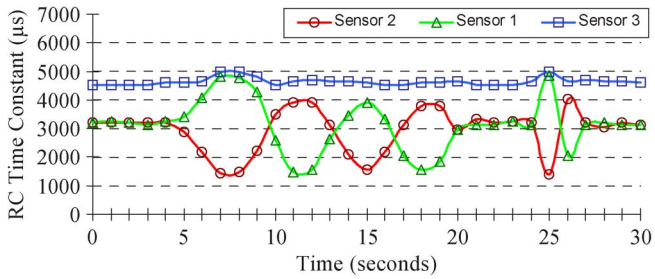

Fig. 26. Sensor data of robot foot when the robot has one-leg balance control. [Robot turns back itself (5–20 s) and human pushes front side (25 s).]

2) Controlled Case: The experiment aims to show two successful example of the balance control of the robot. One is the same unbalanced situation as the failure case. In this case, although the robot turned its body to the back side by itself the same as the previous experiment, the robot could keep its balance. The other is the unbalanced situation caused by the human. In this experiment, human pushed the robot from the front side to realize human–machine interaction. The robot also could balance its body despite the disturbance from the human. Fig. 24 shows the actual movement when the robot turns to the back side by itself. Fig. 25 shows actual movement when the robot interacts with human when human pushes the robot from the front side. Fig. 26 shows the sensing data of this experiment. In this procedure, we first set the robot stand with only left leg in 2 s for initializing the sensing values as shown in Fig. 24(a), and between 0 and 2 s in Fig. 26. Then, the robot starts to turn its body into the back side like the previous experiment to make the robot unbalanced, as shown in Fig. 24(b) and 5 s in Fig. 26. From 5 to 7 s, the robot moved to the back until it reached 3°. After that, the robot reacted to keep its balance based on the sensor values, which is different from the initial sensing values. Hence, the minimum angle that can be detected is 3° for this balancing case. From 8 s in Fig. 26, the robot began turning its body against the internal movement by utilizing the analyses of the distributed pressure patterns. In this case, the outputs of the sensor elements are constrained as follows:

$$SL_2 > SL_3 \geq SL_1. \tag{7}$$

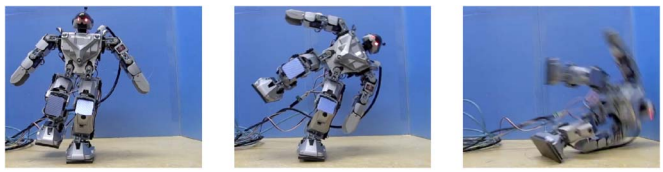

(a) (b) (c)

Fig. 27. Actual movement when the robot turns left. (Without balance control.)

Based on the sensor values, to make the foot normal to the ground surface, the robot needs to move its body front until the robot turned to the balance position again at 10 s in Fig. 26. However, the robot is still moving to reach 20°. Thus, the humanoid robot repeatedly turns its body to keep balance as shown at 13, 17, and 20 s in Fig. 26. Finally, the robot turned to the balance position again where the receiving forces on sensor 1 and 2 are equal, as shown in Fig. 24(c). The robot keeps the balance from this point. The next experiment aims to show that the proposed system enables us to realize human–machine interaction in case that human pushes the robot from the front side. A human then applied the pushing force from the front of robot body by using his finger, as shown in Fig. 25(a), and at 25 s in Fig. 26. The force from the human makes the robot unbalanced. At this state, the robot body began turning by utilizing the analyses of the distributed pressure patterns as described in (7). Based on the sensor values, to make the force on sensor 1 and 2 equal, the robot moves front against human, as shown in Fig. 25(b), and at 26 s in Fig. 26. Then, human leaves their finger out of the robot and the robot still maintains the balance position without falling down, as shown in Fig. 25(c), and at 27 s in Fig. 26. As shown in these figures, the robot also could keep its body based on the balance control in spite of the disturbance from the internal and external forces.

E. Experiment on Robot Balance Actions (Weight on Right Side)

1) Uncontrolled Case: This experiment aims to show the failed example of the robot when the robot turn its body to the right side without proposed method. In this procedure, first we set the robot balance with only the left leg. Then, the robot turns its body into the right side by 1° until 20° to make the robot unbalanced. As a result, after the robot turn to the right without balance control, the robot fell down to this direction, as shown in Fig. 27(a)–(c), respectively.

2) Controlled Case: The experiment aims to show two successful example of the balance control of the robot. One is the same unbalanced situation as the failure case. In this case, although the robot turned its body to the right side by itself the same as the previous experiment, the robot could keep its balance. The other is the unbalanced situation caused by the human. In this experiment, human pushed the robot from the left side to realize human–machine interaction. The robot also could balance its body despite the disturbance from the human. Fig. 28 shows the actual movement when the robot turns to the right side by itself. Fig. 29 shows actual movement when the robot interacts with human when human pushes the robot from the left side. Fig. 30 shows the sensing data of this experiment.

(a) (b) (c)

Fig. 28. Actual movement when the robot turns left. (With balance control.)

(a) (b) (c)

Fig. 29. Actual movement when the robot interacts with human. (Push from the right side.)

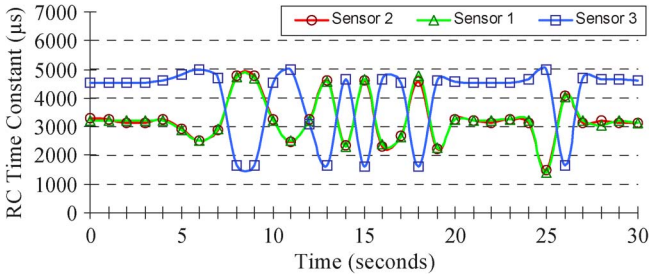

Fig. 30. Sensor data of robot foot when the robot has one-leg balance control. [Robot turns left itself (5–20 s) and human pushes right side (25 s).]

In this procedure, we first set the robot stand with only left leg in 2 s for initializing the sensing values as shown in Fig. 27(a), and between 0 and 2 s in Fig. 30. Then, the robot starts to turn its body into the right side the same as previous experiment to make the robot unbalanced, as shown in Fig. 27(b) and 5 s in Fig. 30. From 5 to 6 s, the robot moved to the right until it reached 2°. After that, the robot reacted to keep its balance based on the sensor values, which is different from the initial sensing values. Hence, the minimum angle that can be detected is 2° for this balancing case. From 6 s in Fig. 30, the robot began turning its body against the internal movement based on the analyses of the distributed pressure patterns. In this case, the outputs of the sensor elements are constrained as follows:

$$(SL_1 \approx SL_2) < SL_3. \tag{8}$$

Based on the sensor values, to make the foot normal to the ground surface, the robot needs to move its body left until the robot turned to the balance position again at 8 s in Fig. 30. However, the robot is still moving to reach 20°. Thus, the humanoid robot repeatedly turns its body to keep its balance as shown at 10, 12, 14, 15, 16, 18, 19, and 20 s in Fig. 30. Finally, the robot turned to the balance position again, as shown in Fig. 28(c). The robot keeps the balance from this point. The next experiment aims to show that the proposed system enables us to realize human–machine interaction in case that human pushes the robot from the left side. A human then applied the pushing force from the left of robot body by using his finger, as shown in Fig. 29(a),

(a) (b) (c)

Fig. 31. Actual movement when the robot turns right. (Without balance control.)

(a) (b) (c)

Fig. 32. Actual movement when the robot turns right. (With balance control.)

and at 25 s in Fig. 30. The force from the human make the robot unbalanced. At this state, the robot body began turning by utilizing the analyses of the distributed pressure patterns as described in (8). Based on the sensor values, to make the robot balance, the robot move left against human, as shown in Fig. 29(b), and at 26 s in Fig. 30. Then, human leaves their figure out of the robot and the robot still maintains the balance position without falling down, as shown in Fig. 29(c), and at 27 s in Fig. 30. As shown in these figures, the robot also could keep its body based on the balance control in spite of the disturbance from the internal and external forces.

F. Experiment on Robot Balance Actions (Weight on Left Side)

1) Uncontrolled Case: This experiment aims to show the failed example of the robot when the robot turn its body to the left side without the proposed method. In this procedure, we first set the robot balance with only the left leg. Then, the robot turns its body into the left side by 1° until 20° to make the robot unbalanced. As a result, after the robot turn to the left without balance control, the robot fell down to this direction, as shown in Fig. 31(a)–(c), respectively.

2) Controlled Case: The experiment aims to show two successful example of the balance control of the robot. One is the same unbalanced situation as the failure case. In this case, although the robot turned its body to the left side by itself the same as the previous experiment, the robot could keep its balance. The other is the unbalanced situation caused by the human. In this experiment, human pushed the robot from the right side to realize human–machine interaction. The robot also could balance its body despite the disturbance from the human. Fig. 32 shows the actual movement when the robot turns to the left side by itself. Fig. 33 shows actual movement when the robot interacts with human when human pushes the robot from the right side. Fig. 34 shows the sensing data of this experiment. In this procedure, we first set the robot stand with only left leg in 2 s for initializing the sensing values as shown in Fig. 32(a), and between 0 and 2 s in Fig. 34. Then, the robot starts to turn its body into the left side like the previous experiment to make

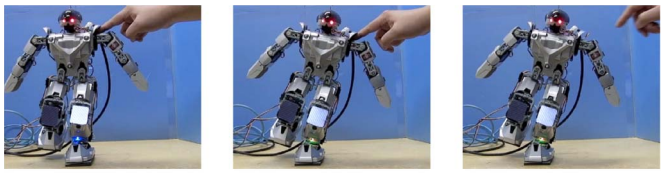

(a) (b) (c)

Fig. 33. Actual movement when the robot interacts with human. (Push from the left side.)

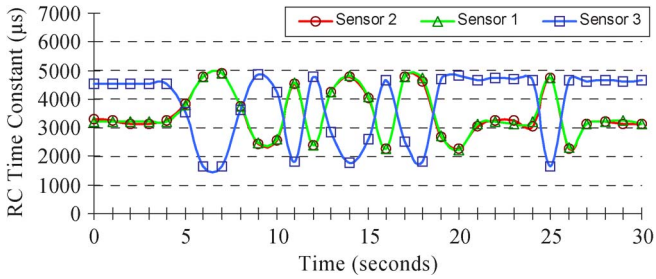

Fig. 34. Sensor data of robot foot when the robot has one-leg balance control. [Robot turns right itself (5–20 s) and human pushes left side (25 s).]

the robot unbalanced, as shown in Fig. 32(b) and 5 s in Fig. 34. From 5 to 6 s, the robot moved to the left until it reached 2°. After that, the robot reacted to keep its balance based on the sensor values, which is different from the initial sensing values. Hence, the minimum angle that can be detected is 2° for this balancing case. From 6 s in Fig. 34, the robot began turning its body against the internal movement by utilizing the analyses of the distributed pressure patterns. In this case, the outputs of the sensor elements are constrained as follows:

$$(SL_1 \approx SL_2) > SL_3. \tag{9}$$

Based on the sensor values, to make the foot normal to the ground surface, the robot needs to move its body right until the robot turned to the balance position again at 8s in Fig. 34. However, the robot is still moving to reach 20°. Thus, the humanoid robot repeatedly turns its body to keep its balance as shown at 8, 10, 11, 13, 15, 16, 19, and 21 s in Fig. 34. Finally, the robot turned to the balance position again, as shown in Fig. 32(c). The robot keeps the balance from this point. The next experiment aims to show that the proposed system enables us to realize human–machine interaction in case that human pushes the robot from the right side. A human then applied the pushing force from the right of robot body by using his finger, as shown in Fig. 33(a), and at 25 s in Fig. 34. The force from the human makes the robot unbalanced. At this state, the robot body began turning by utilizing the analyses of the distributed pressure patterns as described in (9). Based on the sensor values, to make the robot balance, the robot moves left against human, as shown in Fig. 33(b), and at 26 s in Fig. 34. Then, human leaves their finger out of the robot and the robot still maintains the balance position without falling down, as shown in Fig. 33(c), and at 27 s in Fig. 34. As shown in these figures, the robot also could keep its body based on the balance control in spite of the disturbance from the internal and external forces.

VI. Conclusion and Future Works

A new haptic foot system for humanoid robot was presented. The proposed sensors were implemented on two robotic feet. Each foot consists of three thin sheets of force sensitive resistors arranged triangularly with the peripheral circuits. We also showed various experimental results to confirm the ability of the proposed system with two main implementations:

One is an active tactile sensing technique to estimate the ground slope orientation at the specific contact point and then move the robot foot normal to the ground surface for active ground slope recognition. As a result, we succeeded in automatic detection of the ground slope such as flat level surface, up, down, left and right slopes with 20° each.

The other is an active tactile sensing technique to estimate the strongest force position under the foot for balancing its body with one leg, which can be used for human–robot interaction. As a result, we also succeeded in the automatic control to balance its body with one leg without falling down in spite of the robot motion itself and the external force such as the pushing force by the human.

The minimum angle that can be detected for balancing on the front and back side is 3° while the minimum angle that can be detect for balancing on the left and right side is 2°. In these applications, we did not need any information about the contacted ground slope or orientation in advance. The proposed system can be independent from the control of robot body to make the distributed control system. Therefore, we are free from the balancing problem in the robot motion planning and human–robot force interaction.

For future works, we would like to utilize the proposed tactile sensor technique not only to control the foot pose or balance control but also to keep the dynamic balance during the walking motion for biped walking in unstructured environment. We also would like to apply the proposed method to make human–robot interaction tasks more useful and flexible.

References

[1] P. Vadakkepat, P. Lim, L. C. De Silva, L. Jing, and L. Ling, "Multimodal approach to human-face detection and tracking," *IEEE Trans. Ind. Electron.*, vol. 55, no. 3, pp. 1385–1393, Mar. 2008.

[2] B. Jensen, N. Tomatis, L. Mayor, A. Drygajlo, and R. Siegwart, "Robots meet humans-interaction in public spaces," *IEEE Trans. Ind. Electron.*, vol. 52, no. 6, pp. 1530–1546, Dec. 2005.

[3] H. Iwata and S. Sugano, "Human–robot-contact-state identification based on tactile recognition," *IEEE Trans. Ind. Electron.*, vol. 52, no. 6, pp. 1468–1477, Dec. 2005.

[4] C. Fu and K. Chen, "Gait synthesis and sensory control of stair climbing for a humanoid robot," *IEEE Trans. Ind. Electron.*, vol. 55, no. 5, pp. 2111–2120, May 2008.

[5] E. Ohashi, T. Aiko, T. Tsuji, H. Nishi, and K. Ohnishi, "Collision avoidance method of humanoid robot with arm force," *IEEE Trans. Ind. Electron.*, vol. 54, no. 3, pp. 1632–1641, Jun. 2007.

[6] K. Löffler, M. Gienger, and F. Pfeiffer, "Sensors and control concept of a biped robot," *IEEE Trans. Ind. Electron.*, vol. 51, no. 5, pp. 972–980, Oct. 2004.

[7] F. J. Berenguer and F. M. Monasterio-Huelin, "Zappa, a quasi-passive biped walking robot with a tail: Modeling, behavior, and kinematic estimation using accelerometers," *IEEE Trans. Ind. Electron.*, vol. 55, no. 9, pp. 3281–3289, Sep. 2008.

[8] H. Minakata, H. Seki, and S. Tadakuma, "A study of energy-saving shoes for robot considering lateral plane motion," *IEEE Trans. Ind. Electron.*, vol. 55, no. 3, pp. 1271–1276, Mar. 2008.

[9] M. Rucci and P. Dario, "Active exploration procedures in robotic tactile perception," in *Proc. Intell. Robot. Syst.*, 1993, pp. 20–24.

[10] P. Dario and M. Rucci, "Tactile sensors and the gripping challenge," *IEEE Spectr.*, vol. 22, no. 8, pp. 46–52, Aug. 1985.
[11] P. Dario, A. Sabatini, B. Allotta, M. Bergamasco, and G. Buttazzo, "A fingertip sensor with proximity, tactile and force sensing capabilities," in *Proc. IEEE Int. Workshop Intell. Robots Syst.*, 1990, pp. 883–889.
[12] H. Maekawa, K. Tanie, and K. Komoriya, "Dynamic grasping force control using tactile feedback for grasp of multifingered hand," in *Proc. IEEE Int. Conf. Robot. Autom.*, 1996, pp. 2462–2469.
[13] J. Jockusch, J. Walter, and H. Ritter, "A tactile sensor system for a three-fingered robot manipulator," in *Proc. IEEE Int. Conf. Robot. Autom.*, 1997, pp. 3080–3086.
[14] H.-Y. Yoa, V. Hayward, and R. E. Ellis, "A tactile magnification instrument for minimally invasive surgery," in *Proc. 7th Int. Conf. Med. Image Comput. Comput.-Assisted Intervention*, 2004, pp. 89–96.
[15] M. E. Tremblay and M. R. Cutkosky, "Estimating friction using incipient slip sensing during a manipulation task," in *Proc. IEEE Int. Conf Robot. Autom.*, 1993, pp. 429–434.
[16] Y. Yamada, T. Morizono, Y. Umetani, and H. Takahashi, "Highly soft viscoelastic robot skin with a contact object-location-sensing capability," *IEEE Trans. Ind. Electron.*, vol. 52, no. 4, pp. 960–966, Aug. 2005.
[17] R. Hikiji and S. Hashimoto, "Hand-shaped force interface for human-cooperative mobile robot," in *Proc. Int. Workshop Haptic Human-Comput. Interaction*, 2000, pp. 113–118.
[18] T. Maeno and T. Kawamura, "Geometry design of an elastic finger-shaped sensor for estimating friction coefficient by pressing an object," in *Proc. IEEE Int. Conf. Robot. Autom.*, 2003, pp. 1533–1538.
[19] R. Kikuuwe and T. Yoshikawa, "Recognizing surface properties using impedance perception," in *Proc. IEEE Int. Conf. Robot. Autom.*, 2003, pp. 1539–1544.
[20] F. Castelli, "An integrated tactile-thermal robot sensor with capacitive tactile array," *IEEE Trans. Ind. Appl.*, vol. 38, no. 1, pp. 85–90, Jan./Feb. 2002.
[21] H. Hiraishi, N. Suzuki, M. Kaneko, and K. Tanie, "An object profile detection by high resolution tactile sensor using an optical conductive plate," in *Proc. Annu. Conf. Ind. Electron. Soc.*, 1988, pp. 982–987.
[22] G. Murali Krishna and K. Rajanna, "Tactile sensor based on piezoelectric resonance," *IEEE Sensors J.*, vol. 4, no. 5, pp. 691–697, Oct. 2004.
[23] T. Matsunaga, K. Totsu, M. Esashi, and Y. Haga, "Tactile display for 2-D and 3-D shape expression using SMA micro actuators," in *Proc. IEEE Annu. Int. Conf. Microtechnol. Med. Biol.*, 2005, pp. 88–91.
[24] T. Tsuji, Y. Kaneko, and S. Abe, "Whole-body force sensation by force sensor with shell-shaped end-effector," *IEEE Trans. Ind. Electron.*, vol. 56, no. 5, pp. 1375–1382, May 2009.
[25] K. Suwanratchatamanee, M. Matsumoto, R. Saegusa, and S. Hashimoto, "A simple tactile sensor system for robot manipulator and object edge shape recognition," in *Proc. 33rd IEEE Annu. Int. Conf. Ind. Electron. Soc.*, 2007, pp. 245–250.
[26] K. Suwanratchatamanee, M. Matsumoto, and S. Hashimoto, "A simple robotic tactile sensor for object surface sensing," *Adv. Robot.*, vol. 22, no. 8, pp. 867–892, 2008.
[27] K. Suwanratchatamanee, M. Matsumoto, and S. Hashimoto, "A tactile sensor system for robot manipulator and continuous object edge tracking," in *Proc. 7th France-Jpn., 5th Eur.-Asia Congr. Mechatronics*, 2008.
[28] K. Suwanratchatamanee, M. Matsumoto, and S. Hashimoto, "Human–machine interaction through object using robot arm with tactile sensors," in *Proc. 17th IEEE Int. Symp. Robot Human Interactive Commun.*, 2008, pp. 683–688.
[29] K. Suwanratchatamanee, M. Matsumoto, and S. Hashimoto, "A novel tactile sensor torch system for robot manipulator and object edge tracking," in *Proc. 34th IEEE Annu. Conf. Ind. Electron. Soc.*, 2008, pp. 2617–2622.
[30] K. Suwanratchatamanee, M. Matsumoto, and S. Hashimoto, "Tactile/haptic sensor for robots and applications," in *Proc. IEEE Int. Student Exp. Hands-on Project Competition Via Internet Intell. Mechatronics Autom., Internet Conf.*, 2008.
[31] K. Suwanratchatamanee, M. Matsumoto, and S. Hashimoto, "A simple tactile sensing foot for humanoid robot and active ground slope recognition," in *Proc. 5th IEEE Int. Conf. Mechatronics*, 2009, CD-ROM.
[32] K. Suwanratchatamanee, M. Matsumoto, and S. Hashimoto, "Balance control of robot and human–robot interaction with haptic sensing foots," in *Proc. 2nd IEEE Int. Conf. Human Syst. Interaction*, 2009, pp. 68–74.
[33] Texscan Inc., FlexiForce User Manual, Boston, MA, May 2, 2009. [Online]. Available: http://www.tekscan.com/pdfs/FlexiforceUserManual.pdf

Kitti Suwanratchatamanee (S'07) received the B.Eng. degree in electronics and telecommunications engineering from King Mongkut's University of Technology Thonburi, Bangkok, Thailand, in 2002, the M.Eng. degree in electronics engineering from RMIT University, Melbourne, Australia, in 2004, and the Dr.Eng. degree in pure and applied physics (information engineering) from the Graduate School of Science and Engineering, Waseda University, Tokyo, Japan, in 2010.

From 2008 to 2010, he was a Research Fellow of the Japan Society for the Promotion of Science (DC2: 20-56621). He is currently a Research Associate in the Department of Pure and Applied Physics, Waseda University. His research interests are in robotics and automation, including sensors, tactile and haptic sensing systems, robot protocol, industrial robots, humanoid robots, and intelligent welding systems.

Dr. Suwanratchatamanee is a student member of the Robotics Society of Japan. He was the recipient of the IECON'07 Student Scholarship Award, the HCIMA'08 Third-Prize Award, and the HSI'09 Best Paper Award in the area of intelligent systems from IEEE in 2007, 2008, and 2009, respectively.

Mitsuharu Matsumoto (M'06) received the B.Eng. degree in applied physics and the M.Eng. and Dr.Eng. degrees in pure and applied physics from Waseda University, Tokyo, Japan, in 2001, 2003, and 2006, respectively.

He is currently an Assistant Professor with the Education and Research Center for Frontier Science, The University of Electro-Communications, Tokyo. He has published 13 books and more than 50 papers in refereed internal conferences and journals. His research interests are including array signal processing, blind source separation, image processing, optical device, pattern recognition, self-assembly, and robotics.

Dr. Matsumoto received the Ericsson Young Scientist Award from Nippon Ericsson K.K, Japan, in 2009. He is a member of the Institute of Electronics, Information and Communication Engineers.

Shuji Hashimoto (M'09) received the B.S., M.S., and Dr. Eng. degrees in applied physics from Waseda University, Tokyo, Japan, in 1970, 1973, and 1977, respectively.

He is a Professor with the Department of Applied Physics and currently the Dean of the School of Science and Engineering, Waseda University. Since 2000, he has been a Director of the Humanoid Robotics Institute, Waseda University. He is the author of over 400 technical publications, proceedings, editorials, and books. His research interests include human communication and "KANSEI" information processing, including: image processing, music systems, neural computing, and humanoid robotics.

Dr. Hashimoto is a member of the International Computer Music Association, the Institute of Electronics, Information and Communication Engineers, the Information Processing Society of Japan, the Society of Instrument and Control Engineers, the Institute of Systems, Control and Information Engineers, the Institute of Image Electronics Engineers of Japan, the Robotics Society of Japan, the Human Interface Society of Japan, and the Virtual Reality Society of Japan.